Effect of the Transition to Improved Core Confinement Observed in the LHCD Experiment at FT-2 Tokamak

S.I. Lashkul, A.B. Altukhov, A.D. Gurchenko, E.Z. Gusakov, V.V. Dyachenko, L.A. Esipov, M.A. Irzak, M.Yu. Kantor, D.V. Kouprienko, A.A. Perevalov[1], A.N. Saveliev, S.V. Shatalin[1]

Ioffe Institute, Politekhnicheskaya 26, St.Petersburg, Russia

[1]St. Petersburg State Polytekhnical University, Politekhnicheskaya 29, St.Petersburg, Russia

E-mail: Serguey.Lashkul@mail.ioffe.ru

Abstract. To explain a relatively good efficiency of LHCD and improved core confinement transition obtained at the small FT-2 tokamak (R=0.55m, a=0.08m, $B_T \leq 3$T, I_{pl} = 35kA, f_0 = 920MHz, Δt_{pl} = 50ms, Δt_{RF} = 5ms ÷ 12ms) a thorough modeling of experimental data has been performed. Effect of LHW on the transition into improved core confinement regime is discussed in the deuterium plasma experiment. It was observed, that in the LHCD experiment with initial OH density $\langle n_e \rangle = 1.6\ 10^{19}$ m^{-3} the central electron temperature $T_e(r = 0$ cm) measured by laser TS diagnostics increases during RF pulse from 550eV to 700eV and that is accompanied by the density rise and cooling of the plasma periphery. The effect of the density rise could not be explained by increase of working gas or impurity recycling because the D_β line intensity and radiation losses during RF pulse is not appreciably changed. According to GRILL3D, FRTC and ASTRA codes modeling the increase of the density and electron temperature T_e inside of r < 3cm (despite the decrease of ohmic heating power P_{OH} at LHCD) happens due to strong reduction of the electron transport in this region where the magnetic shear vanishes, and the value of thermal diffusivity $\chi_{e,eff}$ decreases. Broadening of the plasma current profile by noninductive LHCD results in flattening of the safety factor q - profile in the plasma column center. As the result, the magnetic shear $s = (r/q)(dq/dr)$ in the center became low, or even negative. In such a case the transport code (where the electron transport was described by the mixed Bohm and gyro-Bohm model) predicts a reduction of the transport. Paper presents new experimental data and modeling results appropriate to the transition to improved core confinement during LHCD experiment. In particular, special attention one attends to the experimental periphery data and data of the threshold power for transition to improved core confinement in deuterium plasma.

1. Introduction

Development of quasi-stationary non-inductive plasma current drive methods in a tokamak is critically important for a thermonuclear reactor [1]. Current drive by lower hybrid waves (LHCD) is the most effective method to sustain the plasma current and there modification, which permits to perform regimes with producing a decrease of the magnetic shear in the region of the power deposition and a local reduction of the thermal electron transport (ITB) in the low or negative shear region [2, 3]. The reduction of the thermal diffusivity through the decrease of shear is accompanied by strong central heating with producing of the high pressure gradient. That modification also is attractive for ITER plasma scenario.

In the present work the main attention is paid to the investigation of this effect on the FT-2 tokamak (R_0=0.55 m, a=0.08 m, $B_T \leq 3T$, I_p=19÷40 kA, Δt_{pl} = 50 ms, Δt_{RF} = (5÷10) ms, f_o = 920MHz, P_{RF}<200kW), where a large experience in the observation of plasma–LH wave interaction has been accumulated and the long-continued experimental run on LHCD efficiency study has been realized [4, 5]. The goal of this paper is to quantify the reduction of anomalous electron transport and the link between the electron transport and the q-profile. The main experimental conditions and methods used in our analyses are described in section

2. In the section 3 the characteristics of the plasma parameters changes during of the LHCD experiment are analyzed in comparing with data of others larger tokamaks. Effect of central electron heating LHCD generation in deuterium plasma is presented in section 4. Modeling and discussion of the experimental data is devoted the section 5. Finally, section 6 contains a summary of this study.

2. The main experimental conditions and methods

In the steady_state phase of the discharge, the RF power at the frequency $f = 920$ MHz was input from the low field side by using a two waveguide grill. Plasma current stabilization was provided by the artificial long line forming the FT-2 discharge pulse. In this case, the LHCD effect manifests itself in the reduction of the loop voltage by the value ΔU_{pl}, which is proportional to the generated current I_{RF}. Multi-Pass Intra-Cavity Thompson Scattering Laser (TS), Neutral Particle Analyzer (NPA), hard X ray (HXR) and soft X ray (SXR), spectroscopic and bolometric diagnostic are used for measurements of experimental data. The indirect characteristics of the superthermal (ST) and runaway electrons (RE) generated during LHCD and forming I_{RF} can be obtained from HXR bremsstrahlung wall radiation diagnostics, which measure gamma quantum's with energy $E_\gamma > 0.2$ MeV [6]. ST and RE electrons energy spectra revealed the generation of electrons with maximal energies about 4 MeV and characteristic energies located in the region from 0.5 to 2.5 MeV. After RF pulse there are shift of the maximal energy of EDF by higher U_{OH} to 5.5 MeV the same as characteristic energy to 3MeV.

3. Comparing the LHCD efficiency with data obtained in others larger tokamaks

In spite of non large dimensions of the FT-2 tokamak and comparatively modest plasma

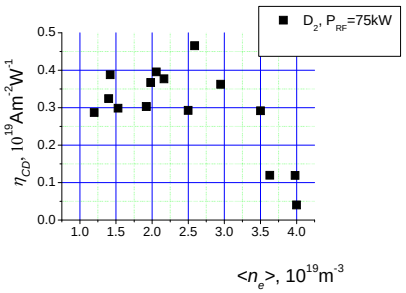

FIG. 1.Efficiency $\eta_{CD} = I_{RF}^N <n_e>$ for deuterium and hydrogen plasmas. $I_{pl} = I_{RF} + I_{OH} = 35$kA, $<T_e> = 390$eV and $Z_{eff} \approx 2$.

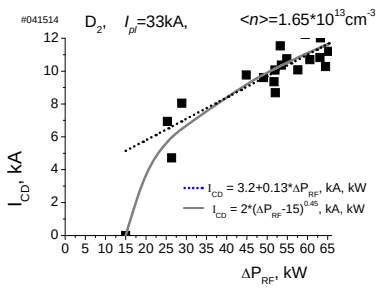

FIG. 2. The relationship between I_{RF} and ΔP_{RF} measured at $I_{pl} = 35$kA and $<n_e> = 1.6\ 10^{19}\ m^{-3}$ revealed the approximately linear relation I_{RF} with ΔP_{RF} (or $I_{RF} \sim \Delta P_{RF}^{\alpha}$, where $\alpha = 0.45$ for deuterium plasma).

parameters [4, 5] the functional dependence and values of efficiency $\eta_{CD} = I_{RF}^N <n_e>$ and $I_{RF}^N = I_{RF}R/P_{RF}$ - normalized LHCD turned out to be close to those obtained in larger tokamaks [7, 8]. Here $I_{RF} = \Delta U\, I_{OH}/U_{OH}$ is LH current drive, $\Delta U = U_{OH} - U_{RF}$, P_{RF} is the LH power and R is the tokamak major radius. The result of measurements of η_{CD} for deuterium plasma at $I_{pl} = I_{RF} + I_{OH} = 35$ kA, $<T_e> = 390$eV and $Z_{eff} \approx 2$ are presented in Fig. 1. As one can see, $\eta_{CD} \approx 0.4\ 10^{19} \mathrm{Am^{-2}W^{-1}}$ for $<n_e> = 1.5\ 10^{19}\ \mathrm{m^{-3}} \div 2.5\ 10^{19}\ \mathrm{m^{-3}}$ density interval. It correlates with the relation obtained for FTU, TS, JT-60, ASDEX and JET (Fig. 6 in [7]). The study of I_{RF}^N dependence on main plasma parameters revealed the typical increment of I_{RF}^N with increase of I_{pl}, T_e and P_{RF} [8]. For instance, the relationship between I_{RF} and

$\Delta P_{RF}=P_{Rf\,inp}$ - $P_{Rf\,refl}$ measured at I_{pl} = *35kA* and base OH density $<n_e>$= 1.6 10^{19}m^{-3} revealed the approximately linear relation $I_{RF} \sim \Delta P_{RF}$, Fig.2. However, these data are in a good accordance with data obtained on [8] (for Tor Supra, JET, JT-60 and ASDEX) where $I_{RF} \sim P_{RF}^{0.65}$ is power function. Fig. 2 shows our data in view of power function as $I_{RF} \sim \Delta P_{RF}^{\alpha}$ also, where $\alpha = 0.5 \pm 0.1$ for deuterium plasma.

4. Effect of LHW on main deuterium plasma parameters at $<n_e>$= 1.6 10^{19} m^{-3}

Fig. 3 and 4 demonstrate changes of the main plasma parameters such as: plasma current I_{pl};

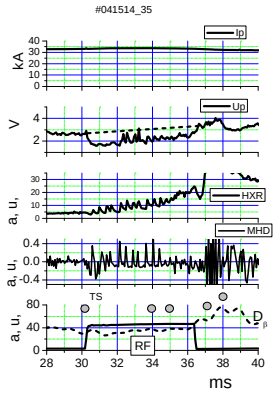

FIG. 3. The waveforms of a typical high power LHW (P_{RF} > 100 KW) discharge: I_{pl}; U_{pl}; HXR; MHD. D_β and P_{RF} Moments of the TS measurements are marked by points

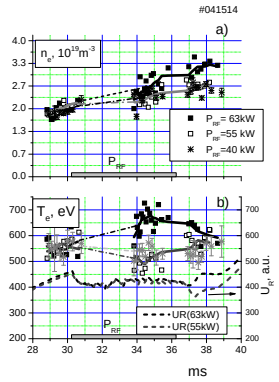

FIG. 4 The variation of the central electron density $n_e(y = 0$ cm) (a) and temperature $T_e(y = 0$ cm) (b) during RF pulse at different ΔP_{RF}. U_R – detector equilibrium signal along of R.

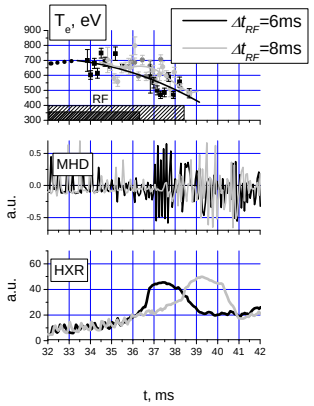

FIG. 5 Effect delay of the high electron temperature mode on elongation of the RF pulse from 6ms to 8ms. MHD activity (m=2, n=1) and HXR signals rise after RF pulse are shifted also

plasma loop voltage U_{pl}; HXR radiation; MHD signal and Dβ line spectral radiation, which are produced by LHW interaction with hot deuterium plasma at the initial density $<n_e>$= 1.6 10^{19} m^{-3} - the density, when effective LHCD is generated, the influence of the parametric decay instability (PDI) effect is low and fast ion generation does not happen [5]. Moments of the electron temperature profile measurements by laser TS diagnostics are marked by points. Dash line on the waveforms of U_{pl} is calculated by ASTRA U_{pl}^{OH} for OH assuming that Z_{eff} increases from 1.5 to 2.5. The U_{pl}^{OH} data need for comparison with U_{pl} for LHCD case. Change of Z_{eff} will be discussed in the next paragraph.

One can see in Fig 4b, that during RF pulse at $\Delta P_{RF} < 60$ kW the central electron temperature $T_e(y = 0$ cm) slightly decreases from 550eV to 500eV and that is accompanied by the central plasma density continuously rises, as shown in Fig. 4a. But at threshold power $\Delta P_{RF}^{th} \approx 63$ kW during RF pulse the electron temperature $T_e(y = 0$ cm) increases from 550eV to 700eV. That high electron temperature mode of $T_e(y = 0$ cm) is held until the end of the 6ms RF pulse. The same result is observed when RF pulse duration is elongated to 8ms, Fig. 5. MHD activity (m=2, n=1) and HXR signals rise after RF pulse is typical effects for LHCD experiments, which are observed in other tokamaks [2]. Accordingly profiles measurements, as one can see in Fig. 6 for $\Delta P_{RF}^{th} \geq 63$kW, the increase of the central electron temperature $T_e(r = 0$ cm) is accompanied by cooling of the plasma periphery, rise and broadening of the density profiles. This effect could not be explained by increase of working gas or impurity

recycling because, the D_β line intensity and radiation losses during RF pulse is not appreciably changed, as one can see in Figures 6 and 7,. Higher radiation losses from the central region are determined by rise of radiation of the most present impurity ions $P_{rad} = \Delta E<n_e><n_{ion}>$, which is determined by the increase in plasma density $<n_e>$ and accumulation of higher ionized impurity $<n_{ion}>$ in the centre of core. So, one can assume that density rise could be explained by particle improved core confinement transition during RF pulse. The new experimental data obtained by spectral HELIOS diagnostics reveal increase of the density gradient near LCFS [9], which verify that proposition. Concurrently the small He admixture in deuterium plasma for diagnostics purpose at periphery permits together with NPA central measurements to obtain data about ion temperature profile change during LHCD generation, which is presented for the same experiment in Fig. 8. Observed additional ion heating at the periphery and middle radii can be result of the Parametric Decay Instability

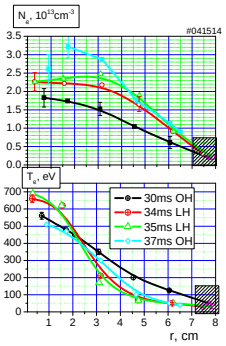

FIG. 6. Evolution of the plasma density $n_e(r)$ and temperature radial profiles $T_e(r)$ measured by TS in the LHCD experiment at $\Delta P_{RF}{}^{th} \approx 63$ kW.

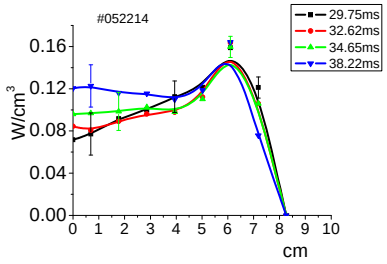

FIG. 7. Evolution of the radiation losses $P_{rad}(r)$ measured by scan pyroelectric bolometer

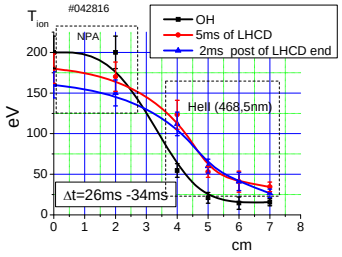

FIG. 8. Evolution of the ion temperature radial profiles measured in the analogous experiment where for diagnostics purpose small He admixture in deuterium plasma is added.

(PDI) of the pumping wave. The increase in density and temperature decrease on the periphery of the discharge contributes to the development of PDI [5]. As to observed spontaneous rise at $\Delta P_{RF} \approx 63$ kW of the central electron temperature $T_e(0)$ only mechanism of improved core confinement (ICC) transition can explain that because heating of bulk plasma electrons during RF pulse ($\Delta t_{RF} = 6$ms) could not be described by collision with LHW generated superthermal and runaway electrons with 200keV÷1MeV energy due to characteristic time $t_E \approx 100 \div 200$ ms >> Δt_{RF}.

5. Modeling and discussion of the LHCD experiment

To explain a relatively good efficiency of LHCD and improved core confinement transition obtained at the small FT-2 tokamak a thorough modeling of experimental data has been performed. The spectrum of the parallel refractive index $N_{//} = N_z$ of LH waves excited in the plasma by the two waveguides antenna was determined using the GRILL3D code [10]. The spectra of the waves $P(N_z)$ are bidirectional (with respect to the plasma current) and have several maxima [4]. For the phase shift between the waveguides $\Delta\varphi = \pi/2$ (asymmetric excitation) there are maxima at $N_z \approx -9$, –1.7 and 3. Using the Fast Ray Tracing Code (FRTC) [11] with the calculated spectrum $P(N_z)$ of LH waves and with the measured plasma parameters, we found the value and direction of LH current. The magnetic equilibrium of the

plasma column was calculated using the ASTRA code. First of all it is necessary to say, that such FRTC modeling revealed the important role of the synergetic effect caused by the interaction of different spectral components of the excited RF waves resulting in "bridging" of the spectral gap [4]. An LH wave with the slowing down factor $N_z = -1.7$ efficiently drives the current only in the presence of slower waves with $N_z = -9$. Radial profiles of LH current drive J_{RF}, MA/m^2 calculated for deuterium plasma using the FRTC code for two values of the plasma density $<n_e> = 1.2\ 10^{19}$m^{-3} and $1.9\ 10^{19}$m^{-3} are presented in Fig. 9. Plasma parameters used for the simulation were the same as those for deuterium plasma with $I_{pl} = 32$kA.

Unfortunately, neither quasi steady electric field nor the impacts of LHCD on the equilibrium plasma parameters were taken into account in these calculations. So, for the estimation of the summary plasma current density profile $(J_{OH}+J_{RF})$ one has to presume that in the experiment with residual vortex toroidal electric field U_{pl} (Fig. 3) the shape of J_{RF} profile is the same as the one presented in Fig. 9a. The values of J_{RF}, J_{OH} and $(J_{OH}+J_{RF})$ in that case can be simulated by ASTRA code modeling on the base of the selected experimental data. The variation of Z_{eff} during the RF pulse shown in Fig. 10 is a linear interpolation between $Z_{eff}(t = 29\text{ms})$ to $Z_{eff}(t = 38\text{ms})$ calculated for ohmic heating stage. Here the comparison of the measured loop voltage $U_{exp}(t)$ and the simulated one $U_{simul}(t)$ is demonstrated. Absolute value of Z_{eff} at each moment of time (for ohmic heating stage) was chosen in such a way that the measured value of the loop voltage $U_{\exp}$ coincides with U_{simul}. Rise of Z_{eff} from 1.5 to 2.2 during the LHW injection reflects decrease of the plasma electro conductivity $\sigma \propto \int_r T_e^{3/2} / Z_{eff} rdr$ because of cooling of the plasma periphery and increase of impurity content of the higher

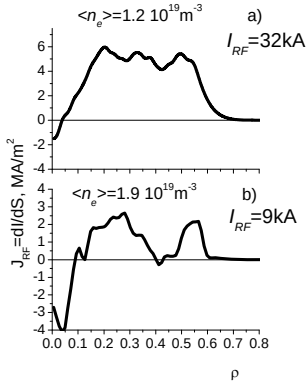

FIG. 9. Radial profiles of LH current drive J_{RF}, MA/m^2 calculated for deuterium plasma using the FRTC code for I_{pl}= 30 kA and two values of the plasma density $<n_e>$. The integral values of I_{RF} are designated.

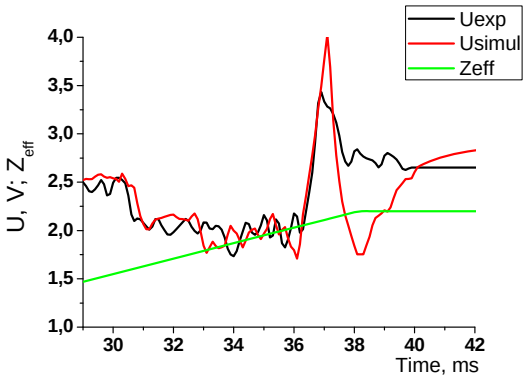

FIG. 10 Variation of Z_{eff} during the RF pulse and comparison of the $U_{exp}(t)$ and simulated $U_{simul}(t)$

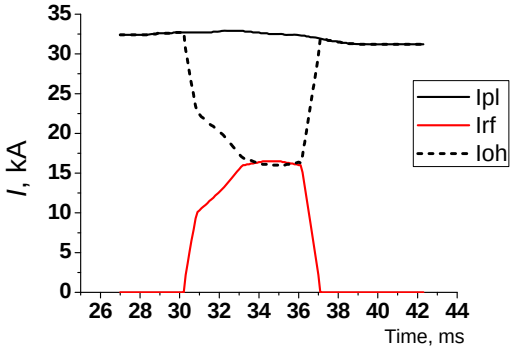

FIG. 11. The values of I_{pl}, calculated as a sum of LH current I_{rf} and residual ohmic current I_{oh}, $(I_{pl} = I_{rf} + I_{oh})$

ionization level (O^{8+} or C^{6+}) due to improved core confinement transition. But impurity

recycling stays at the same level or decreases that follow from D_β line intensity and the radiation losses profiles, as one can see in Figures 3 and 7.

The values of the total current $I_{pl} = I_{rf} + I_{oh}$, calculated as a sum of the LH current I_{rf} and the residual ohmic current I_{oh} are shown in Fig. 11. Shapes of the calculated current density profiles are presented in the Fig. 12, where the summary $J_{sum}(r,t = 34ms) = J_{RF}(r, t = 34ms) + J_{oh}(r, t = 34ms)$ is broader than $J_{oh}(r, t = 30ms)$. The shape of $J_{RF}(r)$ used for draft ASTRA modeling was taken from Fig. 9a, but absolute value of $J_{RF}(r)$ is calculated by ASTRA code through modeling interpolation of the loop voltage presented in Fig. 10.

Broadening of the plasma current profile by noninductive LHCD results in flattening of the safety factor q-profile in the plasma column center. As the result, the magnetic shear

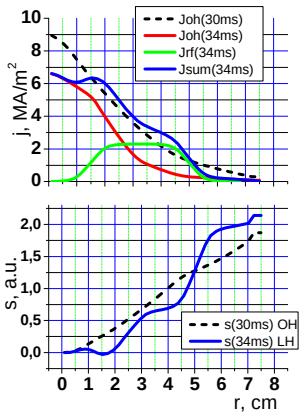

FIG. 12. Shape of the calculated current density profiles, where summary profile at 34ms $J_{sum}(r,t = 34ms) = J_{RF}(r, t = 34ms) + J_{oh}(r, t = 34ms)$. The magnetic shear "s" is presented for two moments (30ms, OH) and (34ms, OH+ RF).

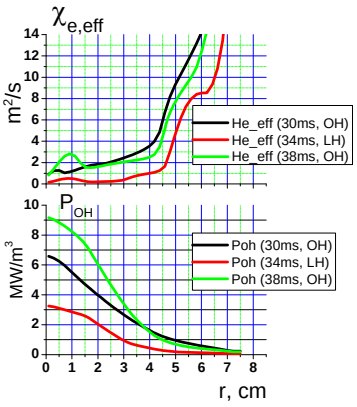

FIG. 13. The profiles of $\chi_{e,\,eff}$ *and* P_{OH} *for three moments of LHCD experiment.*

$s = (r/q)(dq/dr)$ in the center became low, or even negative, Fig. 12. In such a case ($s \sim 0$) at Tore Supra the transport code (where the electron transport was described by the mixed Bohm and gyro-Bohm model) predicts a reduction of the thermal transport [2, 7]. The reduction in transport over the region of low magnetic shear is interpreted as resulting from the toroidal decoupling of the modes, with a subsequent decrease in the radial correlation length of the fluctuations [12].

Following this model one can propose, that the increase of T_e inside r < 3cm (despite the decrease of ohmic heating power P_{oh} at t = 34ms) happens due to the strong reduction of the electron transport in this region where the magnetic shear vanishes, and the value of thermal diffusivity $\chi_{e,\,eff}$ remains significantly below the ohmic level as shown in Fig. 13.

6. Conclusion

The functional dependence and values of LHCD efficiency in deuterium plasma $\eta_{CD} = I_{RF}^{N} \langle n_e \rangle \approx 0.4\ 10^{19} \mathrm{Am^{-2}W^{-1}}$ for $\langle n_e \rangle = 1.5\ 10^{19}\ \mathrm{m^{-3}} \div 2.5\ 10^{19}\ \mathrm{m^{-3}}$ density interval and normalized LHCD I_{RF}^{N} turned out to be close to those which are obtained in larger tokamaks. During RF pulse cooling of the electron temperature and density rise is observed. The central electron temperature $T_e(y = 0\ \mathrm{cm})$ slightly decreases from 550eV to 500eV. But at threshold power $\Delta P_{RF}^{th} = P_{Rf\,input} - P_{Rf\ \ reflect} \geq 63$ kW during RF pulse central electron

temperature $T_e(y = 0$ cm) increases. In this situation at the initial OH density $<n_e> = 1.6\ 10^{19}$ m^{-3} during RF pulse central $T_e(r = 0)$ increases from 550eV to 700eV. It also is accompanied by cooling of the plasma periphery and density rise. Comprehensive GRILL3D, FRTC and ASTRA codes modeling showed that ICC transition happens due to a strong reduction in the electron transport in the $r < 3$cm region resulting from broadening of the plasma current density profile by suprathermal and runaway electrons generated by LHW. When the magnetic shear "*s*" vanishes up to $s = (r/q)(dq/dr) \leq 0$ inside r < 3cm the value of thermal diffusivity χ_{eff} and diffusion factor D_e, accordingly Bohm and gyro-Bohm models, decreases [2, 3, 7]. The residual ohmic power will be enough for additional central electron heating at low background thermal diffusivity χ_{eff}. In such case ICC is observed. But decrease of the heat input at the periphery results in cooling of the electron component here. Periphery cooling at density rise during RF pulse can promote PDI, which result in observed ion heating at periphery and middle radii the same as decreasing of η_{CD} [5].

This work (for S.I. Lashkul and FT-2 team) was supported in part by the Russian Foundation for Basic Research project nos 14-08-00476

References:

[1] M GONICHE, L AMICUCCI , Y BARANOV ET AL., "Lower hybrid current drive for the steady-state scenery", Plasma Phys. Control. Fusion, (2010) 52 124031

[2] X LITAUDON, Y PEYSSON, T ANIEL, ET AL., "*q*-profile evolution and improved core electron confinement in the full current drive operation on Tore Supra", Plasma Phys. Control. Fusion 43 (2001) 677–693

[3] T.J.J. TALA, J. A. HEIKKINEN, V.V. PARAIL ET AL., "ITB formation in terms of ω_{ExB} flow shear and magnetic shear s on JET", Plasma Phys. Control. Fusion 43, 2001, 507 – 523

[4] S.I. LASHKUL, A.B. ALTUKHOV, A.D. GURCHENKO ET AL., "Analysis of the Efficiency of Lower Hybrid Current Drive in the FT-2 Tokamak", 2010 Plasma Physics Reports Vol. 36, No. 9, pp. 751–761

[5] S.I. LASHKUL, A.B. ALTUKHOV, A.D. GURCHENKO, E.Z. ET AL., "Impact of isotopic effect on density limit and LHCD efficiency in the FT-2 experiments", Nucl. Fusion 55 (2015) 073019

[6] A.E. SHEVELEV, E.M. KHILKEVITCH, S.I. LASHKUL ET AL., "High performance gamma-ray spectrometer for runaway electron studies on the FT-2 tokamak", Nuclear Instruments and Methods in Physics Research A830 (2016) 102–108

[7] Y. PEYSSON AND THE TORE SUPRA TEAM, "Progress towards high-power lower hybrid current drive in TORE SUPRA", 2000 Plasma Phys. Control. Fusion 42 B87–B114

[8] V. PERICOLI RIDOLFINI, G. CALABR`O, L. PANACCIONE ET AL., "Study of lower hybrid current drive efficiency over a wide range of FTU plasma parameters" 2005, Nucl. Fusion 45 1386–1395

[9] S.I. LASHKUL, A.B. ALTUKHOV, A.D. GURCHENKO ET AL., "Helium fuelling for edge plasma parameters control in the thermonuclear experiments" 42nd EPS Conference on Plasma Physics, 22 - 26 June *2015*. Lisbon, P5.173

[10] M.A. IRZAK AND O.N. SHCHERBININ, "Theory of Waveguide Antennae for Plasma Heating and Current Drive" (1995) Nucl. Fusion 35 pp.1341–56.[11] D. PILIYA AND

A. N. SAVELIEV., “Numerical Code for LHCD Simulations with
Self- consistent Treatment of Alpha Particles in Tokamak Geometry”, 1998 Preprint (No. JET_R(98) 01, Abingdon, 1998).

[12] ROMANELLI F AND ZONCA F., “The radial structure of the ion-temperature-gradient-driven mode”, 1993 Phys. Fluids B **5** 4081